

# Low-Noise Active-RC Allpole Filters Using Optimized Biquads

UDK 621.372.542:621.375.132  
IFAC 3.1.1; 5.8.0

Original scientific paper

In this paper it is shown that active-RC filters can be designed to have low-sensitivity to passive components and at the same time possess low output thermal noise. The design procedure of low-noise and low-sensitivity, positive-feedback, second- and third-order low-pass allpole filters, using impedance tapering, has already been published. The noise analysis in this paper was extended to the high-pass and band-pass filters and those with negative-feedback. The optimum designs, regarding both noise and sensitivity of most useful filter sections were summarized in the table form (as a cookbook) and demonstrated on examples. The classical methods were used to determine output noise spectral density and total rms output noise of filters. It was found that low-sensitivity filters with minimum noise have reduced resistance levels, low Q-factors, low-noise operational amplifiers and use impedance tapering design.

**Key words:** Low sensitivity, Low noise, Low-, High-, and Band-pass active-RC filters, Single-amplifier biquads, Allpole filters.

**Projektiranje svepolnih aktivnih RC filtara niskog šuma pomoću optimiranih bikvadratnih sekcija.** U ovom radu je prikazano da optimalne aktivne RC filtarske sekcije s niskim osjetljivostima na varijacije pasivnih komponenata istovremeno imaju nizak nivo termičkog šuma na izlazu. Postupak projektiranja nisko osjetljivih i nisko šumnih, nisko-propusnih filtarskih sekcija drugog i trećeg reda s pozitivnom povratnom vezom pomoću 'skaliranja impedancija' je već objavljen. U ovom radu je analiza izlaznog šuma proširena na nove sekcije koje realiziraju pojasno-propusnu i visoko-propusnu frekvencijsku karakteristiku kao i na sekcije koje koriste negativnu povratnu vezu u realizaciji. Svi postupci optimalnog projektiranja u smislu niskog šuma i niske osjetljivosti za najreprezentativnije filtarske sekcije su sažeti i raspoloživi u obliku tablica s postupkom projektiranja 'korak po korak' (kuharica) te pokazani na primjerima. U istraživanju su korištene klasične metode za određivanje spektralne gustoće šuma i totalne efektivne vrijednosti šuma na izlazu filtara. Pokazano je da filtri sa niskim osjetljivostima koji istovremeno imaju nizak nivo šuma posjeduju niske vrijednosti otpora, realiziraju niske Q faktore, koriste niskošumna operacijska pojačala u realizaciji te su projektirana metodom skaliranja impedancija.

**Ključne riječi:** niska osjetljivost, niski šum, nisko-, visoko- i pojasno-propusni aktivni RC filtri, bikvadratne sekcije s jednim pojačalom, svepolni filtri.

## 1 INTRODUCTION

In this paper the relationship between the low sensitivity and low output noise, that are the most important performance of active-RC filters, is investigated. In active-RC filters the noise performance is important because of two reasons: *i*) it is desirable that a signal has a large dynamic range for operation at the output ('output noise' has to be at its minimum); and *ii*) if the low-signal-level and low-power signal has to be recovered from a noise background using active-RC filter, signal-to-noise ratio (SNR) has to be maximized ('input noise' has to be at its minimum). In this paper we present optimum designs that reduce the active filter noise performance.

A considerable improvement in sensitivity of single-amplifier active-RC allpole filters to passive circuit com-

ponents is achieved using the design technique called 'impedance tapering' [1], and as we show here, at the same time they will have low output thermal noise. The improvement in noise and sensitivity comes free of charge, in that it requires simply the selection of appropriate component values. The design of optimal second- and third-order sections referred to as 'biquads' and 'bitriplets', regarding low *passive* and *active* sensitivities has been summarized in the table form as a cookbook in [2]. Low-pass (LP), high-pass (HP) and band-pass (BP) filter types, as well as the filter sections using positive and negative feedback, have been considered. These filters are of low power because they use only one operational amplifier (opamp) per circuit. For common filter types, such as Butterworth and Chebyshev, design tables with normalized component

values for designing single-amplifier LP filters up to the sixth-order with optimized *passive* sensitivity have been presented in [3].

Preliminary results of the investigation of the relation between low sensitivity and low thermal noise performances using impedance tapering on the numeric basis have been presented elsewhere [4, 5]. For LP filters of second- and third-order the complete analytical proofs for noise properties of the desensitized filters are given in [6]. Both the output noise and the sensitivity to component tolerances were subject of the research by many authors [7–11]. By means of classical methods as in [7–11] closed-form expressions are derived in this paper, providing insight into noise characteristics of the LP, HP and BP active-RC filters using different designs. It was shown that both noise and sensitivity are directly proportional to the pole Q's and, therefore, to the pass band ripple specified by the filter requirements. The smaller the required ripple, the lower the pole Q's. Besides, it is wise to keep the filter order  $n$  as low as the specifications will permit, because the lower the filter order, the lower the pole Q's. Also, it was shown that positive-feedback filter blocks are useful for the realization of the LP and HP filters (belonging to class 4, according to the classification in [12], the representatives are SAK: Sallen and Key filters [13]). Filters with negative feedback (class 3 SAB: Single-amplifier Biquad) are better for the BP filters, where the BP-C Biquad is preferable because it has lower noise than BP-R.

In Section 2 output noise and dynamic range are defined as figure-of-merit for noise performance of active-RC filters. In Section 3, noise of the second-order LP, HP and BP (recommended in [2]) Biquads is analyzed. In Section 4, noise of the third-order LP and (dual) HP Biquads (Biotriplets) is analyzed. Section 5 concludes this work.

## 2 NOISE FIGURE-OF-MERIT

There are several origins of noise in electrical circuits that can seriously limit the processing of signals by analog circuits. In this paper we will investigate only the thermal (or Johnson) noise. Thermal noise is result of random fluctuations of voltages or currents. Because, this noise is proportional to the temperature, it is referred to as thermal noise.

Active-RC filters consist of resistors, capacitors and opamps. The most important sources of noise are resistors and opamps. For the purpose of noise analysis, appropriate noise models for resistors and opamps must be used. Because we describe the influence of the stochastic noise generated by resistors using powers, we use squares of voltages or currents.

Resistors are represented by the well-known Nyquist voltage or current noise models shown in Fig. 1(a) and (b),

consisting of noiseless resistors and noise sources whose values are defined by the squared noise voltage density within the narrow frequency band  $\Delta f$  as follows

$$e_{nR}^2(f) = 4kTR [V^2/Hz], \tag{1}$$

or the squared noise current density given by

$$i_{nR}^2(f) = 4kT/R [A^2/Hz], \tag{2}$$

where  $k = 1.38 \cdot 10^{-23}$  (Boltzmann's constant) and we use absolute temperature  $T=295K$  in all examples ( $22^\circ C$  room temperature). The squared noise spectral density in (1) has the dimension  $[V^2/Hz]$ , unless written  $e_{nR}^2(\omega)$  (or without notation ' $\omega$ '), in which case the dimension  $[V^2/rad/s]$  is implied. The same notation is used for (2) with 'A' instead 'V'. The noise defined by (1) and (2) has a constant spectrum over the frequency band, and is referred to as 'white noise'. The noise in real capacitors is also of thermal origin. It is produced within the resistive, non-ideal part of a capacitor, and can generally be neglected.

The noise in operational amplifiers is caused by the built-in semiconductors and resistors. Opamps used in analysis are assumed to be ideal having infinite and constant gain  $A \rightarrow \infty$ , infinite input impedance and zero output impedance. The equivalent schematic of a noisy opamp is shown in Fig. 1(c), that is, a noiseless opamp combined with voltage and current noise sources. For the TL081/TI (Texas instruments) FET input opamp, typical values found in the data-sheets are  $e_{na}(f) = 17nV/\sqrt{Hz}$  and  $i_{na1}(f) \approx i_{na2}(f) = 0.01pA/\sqrt{Hz}$ . These values are considered constant within the frequency interval up to about 50 kHz and have been used in the noise analysis in this article.

The noise sources of resistors and opamps can be considered random and uncorrelated in the frequency band under consideration. Consequently, the noise is additive and the spectral power density of the noise voltage at the output terminal is obtained by adding the contributions from each source.

The evaluation of the total rms noise voltage at the filter output is performed in three steps. First, the *noise transfer function*  $T_k(s) = V_2/N_k$  from each equivalent voltage or current noise source  $n_k^2 = e_{nk}^2$  or  $i_{nk}^2$  of the  $k$ th element

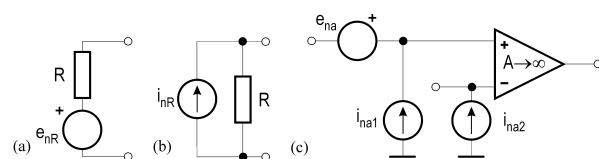


Fig. 1. (a) Voltage noise model of a resistor. (b) Current noise model of a resistor. (c) An opamp noise model

to the output of the filter is evaluated. Then the spectral densities of all these noise effects at the filter output must be summed up to:

$$e_{no}^2(\omega) = \sum_k |T_k(j\omega)|^2 \cdot (n_k)^2, \quad (3)$$

where  $|T_k(j\omega)|$  is modulus of the corresponding voltage transfer function or the transfer impedance, depending on the voltage or current nature of the  $k$ th noise source.

Finally, the total output noise power is obtained by the integration of the mean-square noise spectral density  $e_{no}^2(\omega)$  in (3) over the total frequency band from 0 to  $\infty$ , thus:

$$(E_{no})_{rms}^2 = \int_0^\infty e_{no}^2(\omega) d\omega. \quad (4)$$

The resulting *noise floor*, i.e. the total rms noise voltage at the output, defined by the square root of (4), limits the smallest signal that can effectively be processed, as well as defining the upper useful boundary of signal amplification. For all filter examples in this paper the rms total output noise voltage defined by (4) was calculated analytically and double-checked numerically over the frequency range 1kHz–1MHz using Matlab.

The determination of *dynamic range* of an active-RC filter is, of course, trivial when the output noise level is known [7]. The dynamic range  $D_R$  is then defined by:

$$D_R = 20 \log \frac{(V_{so\ rms})_{max}}{(E_{no})_{rms}} \quad [\text{dB}], \quad (5)$$

where the numerator represents the maximum undistorted rms voltage at the output, and the denominator is the noise floor defined by the square root of (4). The numerator in (5) is determined by the opamp power supply voltage, slew rate, and the corresponding THD factor of the filter. In our examples we use a  $10V_{pp}$  signal which yields  $(V_{so\ rms})_{max} = 5/\sqrt{2}$  [V].

### 3 SECOND-ORDER BIQUADS

Consider the second-order Biquads that realize LP, HP and BP transfer functions, shown in Fig. 2. Those are the Biquads that are recommended in [2] as high-quality building blocks. On the basis of component ratios in the passive, frequency-dependent feedback network of the Biquads in Fig. 2, defined by:

$$\rho = C_1/C_2, r = R_2/R_1, \quad (6)$$

the detailed step-by-step design of those filters, in the form of cookbook, for both optimum *passive* and *active* sensitivities is given in [2] and in Table 1. They are also recommended in [14] as high-quality filter circuits. In [14] only

the design procedure for min. GSP is given (and by that providing the minimum *active* sensitivity design).

Note that the Biquads in Fig. 2 shown vertically are related by the complementary transformation, whereas those shown horizontally are RC–CR duals of each other. Thus, complementary circuits are LP (class-4: positive feedback) and BP-C (class-3: negative feedback), as well as HP (class-4) and BP-R (class-3). In class-4 case there is  $\beta$ , whereas in class-3 there is  $\bar{\beta}$ , that are related by:

$$\beta^{-1} + \bar{\beta}^{-1} = 1. \quad (7)$$

Dual Biquads in Fig. 2 are LP and HP (class-4), as well as BP-C and BP-R (class-3); they belong to the same class.

Voltage transfer functions for the filters in Fig. 2 in terms of the pole frequency  $\omega_p$ , the pole Q,  $q_p$  and the gain factor  $K$ , are given by:

$$T(s) = \frac{V_2}{V_1} = \frac{N(s)}{D(s)} = K \cdot \frac{n(s)}{s^2 + (\omega_p/q_p)s + \omega_p^2}, \quad (8a)$$

where numerators  $n(s)$  are given by:

$$n_{HP}(s) = s^2, \quad n_{BP}(s) = \omega_p \cdot s, \quad n_{LP}(s) = \omega_p^2. \quad (8b)$$

Parameters  $\omega_p$ ,  $q_p$  and  $K$ , as functions of filter components, are given in the first row in Table 2. Note that all filters in Fig. 2 have the same expressions for  $\omega_p$ , and that the expressions for pole Q,  $q_p$  are identical only for complementary circuits. This is the reason why complementary circuits have *identical* sensitivity properties (see the sensitivity expressions in the second and third rows in Table 2), and share the same optimum design.

On the other hand, two 'dual' circuits will have *dual* sensitivities and dual optimum designs. Dual means that the roles of resistor ratios are interchanged by the corresponding capacitor ratios, and vice versa.

Referring to Fig. 2, the voltage attenuation factor  $\alpha$  ( $0 < \alpha \leq 1$ ), which decouples gains  $K$  and  $\beta$  (see [1]), is defined by the voltage divider at the input of the filter circuits.

The Thevenin impedance of the voltage divider is  $R_1 = R_{11}R_{12}/(R_{11} + R_{12})$  or  $C_1 = C_{11} + C_{12}$ . In the limiting case when  $\alpha=1$ , providing  $R_1 = R_{11}$ ,  $R_{12} = \infty$ , or  $C_1 = C_{11}$ ,  $C_{12} = 0$ , and maximum signal gain  $K$ , it has no effect on output noise. The case  $\alpha=1$  is assumed throughout this paper.

In what follows, we investigate and report the optimum design regarding output thermal noise for the filters in Fig. 2. For the second-order LP Biquad in Fig. 2(a) the detailed noise analysis on the analytical basis is given in [6]. The methodology in [6] is used here to extend the low-noise designs to HP and BP Biquads in Fig. 2. Using noise models

Table 1. Optimum step-by-step design procedure for second-order filters in Fig. 2

(a) LP and (c) BP-C	(b) HP and (d) BP-R
i) Choose: $C_1, \rho \gg 1$ (e.g. $\rho=4$ ) [or calculate $C_1=C_{TOT}/(1+1/\rho)$ ].	i) Choose: $C_1, r \gg 1$ (e.g. $r=4$ ) [or calculate $C_1=C_{TOT}/(1+1/\rho)$ ].
ii) Choose: $r=1$ or calculate $r$ for min GSP: $r = \frac{\rho}{36q_p^2} \left[ \sqrt{1+12q_p^2 \left(1 + \frac{1}{\rho}\right)} + 1 \right]^2$	ii) Choose: $\rho=1$ or calculate $\rho$ for min GSP: $\rho = \frac{r}{36q_p^2} \left[ \sqrt{1+12q_p^2 \left(1 + \frac{1}{r}\right)} + 1 \right]^2$
iii) Calculate: $R_1 = \frac{1}{\omega_p C_1} \sqrt{\frac{\rho}{r}}, \beta = 1 + \frac{1+r}{\rho} - \frac{1}{q_p} \sqrt{\frac{r}{\rho}}$	iii) Calculate: $R_1 = \frac{1}{\omega_p C_1} \sqrt{\frac{\rho}{r}}, \beta = 1 + \frac{1+\rho}{r} - \frac{1}{q_p} \sqrt{\frac{\rho}{r}}$
iv) Choose $R_G$ and calculate remaining components (LP filter): $\alpha = K/\beta; R_2 = rR_1; C_2 = C_1/\rho; R_{11} = R_1/\alpha;$ $R_{12} = R_1/(1-\alpha); R_F = R_G(\beta-1).$	iv) Choose $R_G$ and calculate remaining components (HP filter): $\alpha = K/\beta; R_2 = rR_1; C_2 = C_1/\rho; C_{11} = \alpha C_1;$ $C_{12} = (1-\alpha)C_1; R_F = R_G(\beta-1).$
For the BP-C filter we use $\bar{\beta}$ [which is equal to value $\beta$ in step iii)], choose $R_F$ and calculate remaining components: $\alpha = K/(\bar{\beta}q_p) \cdot \sqrt{r/\rho}; R_2 = rR_1; C_2 = C_1/\rho;$ $C_{11} = \alpha C_1; C_{12} = (1-\alpha)C_1; R_G = R_F(\bar{\beta}-1).$	For the BP-R filter we use $\bar{\beta}$ [which is equal to value $\beta$ in step iii)], choose $R_F$ and calculate remaining components: $\alpha = K/(\bar{\beta}q_p) \cdot \sqrt{\rho/r}; R_2 = rR_1; C_2 = C_1/\rho;$ $R_{11} = R_1/\alpha; R_{12} = R_1/(1-\alpha); R_G = R_F(\bar{\beta}-1).$

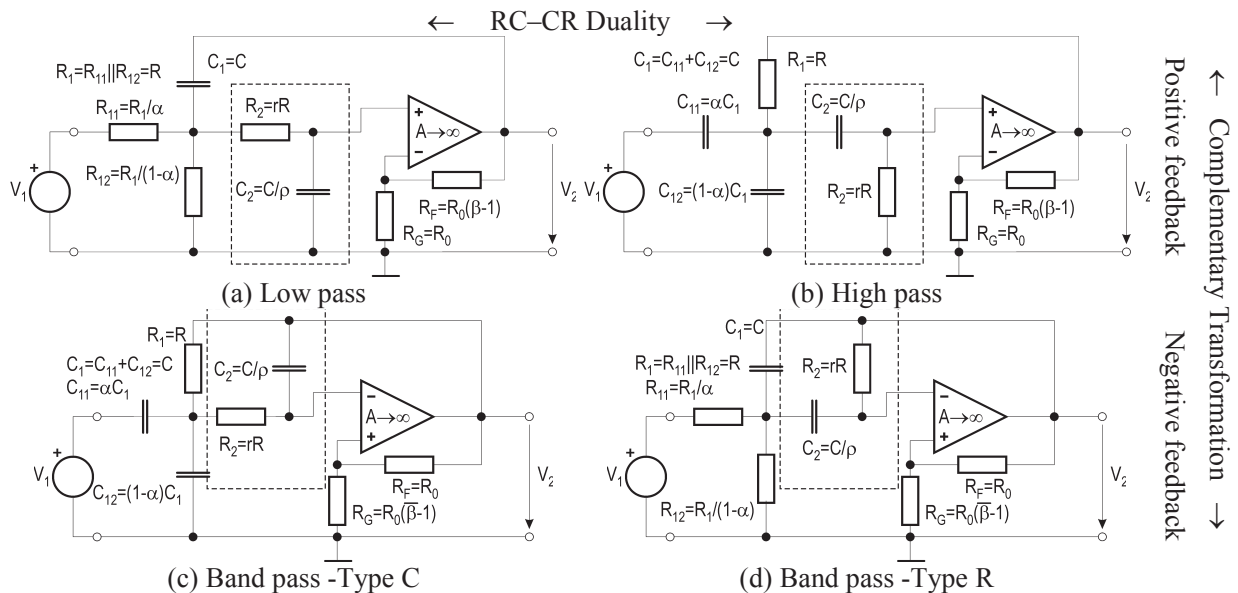


Fig. 2. Second-order LP, HP and BP active-RC filters with impedance scaling factors  $r$  and  $\rho$

for the resistors and opamps, we obtain the configurations shown in Fig. 3.

Inspection of the Fig. 3 shows that complementary Bi-quads have identical noise transfer functions, and therefore the same output noise, because the opamp output has low impedance.

It is common to divide the output noise into two parts: 'passive noise' due to the resistors  $R_1$  and  $R_2$  in the filter's passive-RC network, and 'active noise' due to the amplifier with the accompanying feedback resistors  $R_F$  and  $R_G$ . The contribution from the amplifier noise current sources

$i_{na1}$  and  $i_{na2}$  can often be neglected (especially because the opamp has low-current FETs at the inputs).

Using the equivalent noise models of filters shown in Fig. 3, and the same procedure as in [6], the total output noise power for all Biquads is calculated by integration as in (4) and consists of the three parts, which are given in Table 3. Note that all these quantities are proportional to the resistance level ( $R_1$  and  $R_2$ ), pole Q-factor  $q_p$ , pole frequency  $\omega_p$ , and component ratios.  $\omega_x$  is the maximum bandwidth of the noise measurement equipment, or the post-filtering network. For large  $q_p$  values, we can ne-

Table 2. Transfer function parameters and sensitivities for the filters in Fig. 2

(a) LP and (c) BP-C	(b) HP and (d) BP-R	Filter parameters
$\omega_p = \frac{1}{\sqrt{R_1 R_2 C_1 C_2}}, q_p = \frac{\sqrt{R_1 R_2 C_1 C_2}}{R_1(C_1 + C_2) + R_2 C_2 - \beta R_1 C_1}$ $K = \alpha\beta \text{ for LP and } K = \alpha\beta q_p \sqrt{R_1 C_1 / (R_2 C_2)} \text{ for BP-C.}$	$\omega_p = \frac{1}{\sqrt{R_1 R_2 C_1 C_2}}, q_p = \frac{\sqrt{R_1 R_2 C_1 C_2}}{(R_1 + R_2)C_2 + R_1 C_1 - \beta R_2 C_2}$ $K = \alpha\beta \text{ for HP and } K = \alpha\beta q_p \sqrt{R_2 C_2 / (R_1 C_1)} \text{ for BP-R.}$	
$S_x^{q_p} \approx q_p \cdot \left( \sqrt{\frac{r}{\rho}} + \frac{1}{\sqrt{r\rho}} \right)$	$S_x^{q_p} \approx q_p \cdot \left( \sqrt{\frac{\rho}{r}} + \frac{1}{\sqrt{r\rho}} \right)$	Passive sensitivity <sup>a</sup>
$\text{GSP: } \Gamma_A^{q_p} = A \cdot S_A^{q_p} = q_p \beta^2 \sqrt{\frac{\rho}{r}}$	$\text{GSP: } \Gamma_A^{q_p} = A \cdot S_A^{q_p} = q_p \beta^2 \sqrt{\frac{r}{\rho}}$	Active sensitivity

<sup>a</sup> By  $x$  we denote all passive components in feedback networks (FN).  $i$ ) In frequency dependent FN:  $R_i, C_i, (i=1, 2)$ ; and  $ii$ ) in resistive FN:  $R_G, R_F$ .

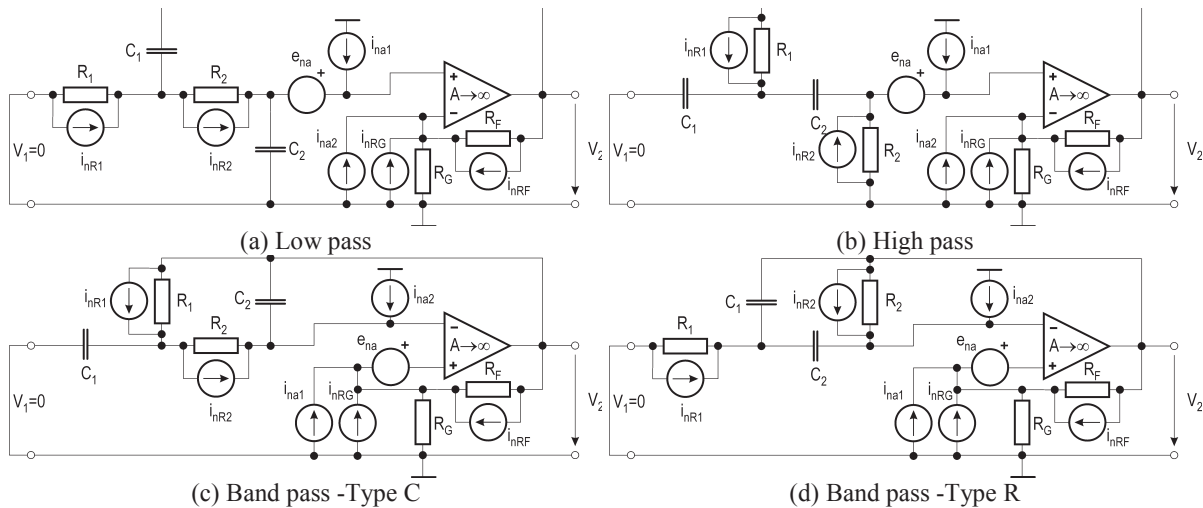


Fig. 3. Noise sources for second-order filters in Fig. 2

glect the influence of the terms with  $\omega_x$ , within the active noise contributions. The total output noise power (4) is given by:

$$E_{no}^2 = E_{nR1R2}^2 + E_{nOA}^2 + E_{nRGRF}^2 \tag{9}$$

### 3.1 Output Noise and Sensitivity Optimization

It is well known that the simplest way to achieve low output noise is to use low-noise opamps and to reduce resistor values to a minimum. Low resistor values require high capacitance values. Therefore, in comparing noise performance of different designs we have to assume that the total capacitance is constant, and equal to some value determined by design constraints such as the technology used, component quality or cost. We choose:

$$C_{TOT} = C_1 + C_2 = 100 \text{ pF.} \tag{10}$$

A trade-off clearly exists between the total chip area (proportional to  $C_{TOT}$ ) and thermal noise (proportional to the resistor values). The feedback resistors are chosen to be  $R_G=10 \text{ k}\Omega$  and  $R_F=R_G(\beta-1)$  (near to the value of  $10 \text{ k}\Omega$ ).

An optimization of both sensitivity and noise performance is possible by varying the general impedance tapering factors (6) of the resistors and capacitors in the passive-RC network of the filters in Fig. 2 (see [1, 2]). By increasing  $r > 1$  and/or  $\rho > 1$ , the  $R_2$  and  $C_2$  impedances are increased. High-impedance sections are surrounded by dashed rectangles in Fig. 2.

To illustrate this, consider the following practical design example as in [1]:

$$\omega_p = 2\pi \cdot 86 \text{ kHz}; \quad q_p = 5; \quad C_{TOT} = 100 \text{ pF.} \tag{11}$$

Table 3. Individual contributions to the total output noise power  $(E_{no})_{rms}^2$  for the filters in Fig. 2

Source	(a) LP and (c) BP-C	(b) HP and (d) BP-R	
$R_1, R_2$	$E_{nR1R2}^2 = \frac{2kT}{\pi} \beta^2 \left[ R_1 + R_2 + R_1 \frac{C_1}{C_2} \right] \cdot \left( \frac{\pi}{2} q_p \omega_p \right)$	$E_{nR1R2}^2 = \frac{2kT}{\pi} \beta^2 \left( 1 + \frac{C_2}{C_1} \right) \left[ R_1 + R_2 + R_1 \frac{C_1}{C_2} \right] \cdot \left( \frac{\pi}{2} q_p \omega_p \right)$	Passive noise
$e_{na}, i_{na1}, i_{na2}$	$E_{nOA}^2 = \left( \beta^2 e_{na}^2 + R_F^2 i_{na2}^2 \left( \frac{1}{\hat{q}^2} - \frac{1}{q_p^2} \right) \right) \cdot \left( \frac{\pi}{2} q_p \omega_p \right) + \beta^2 R_1^2 i_{na1}^2 \left[ \frac{R_2 C_1}{R_1 C_2} + \left( 1 + \frac{R_2}{R_1} \right)^2 \right] \cdot \left( \frac{\pi}{2} q_p \omega_p \right) + \left( \beta^2 e_{na}^2 + R_F^2 i_{na2}^2 \right) \cdot \omega_x$	$E_{nOA}^2 = \left( \beta^2 e_{na}^2 + R_F^2 i_{na2}^2 \left( \frac{1}{\hat{q}^2} - \frac{1}{q_p^2} \right) \right) \cdot \left( \frac{\pi}{2} q_p \omega_p \right) + \beta^2 R_1^2 i_{na1}^2 \left[ \left( \frac{R_2 C_2}{R_1 C_1} - 1 \right) + \frac{R_2 C_1}{R_1 C_2} + \left( 1 + \frac{R_2}{R_1} \right)^2 \right] \cdot \left( \frac{\pi}{2} q_p \omega_p \right) + \left( \beta^2 e_{na}^2 + R_F^2 i_{na2}^2 \right) \cdot \omega_x$	Active noise <sup>a</sup>
$R_G, R_F$	$E_{nRGRF}^2 = \frac{2kT}{\pi} \left[ R_G (\beta - 1)^2 + R_F \left( \frac{1}{\hat{q}^2} - \frac{1}{q_p^2} \right) \right] \cdot \left( \frac{\pi}{2} q_p \omega_p \right) + \frac{2kT}{\pi} \left[ R_G (\beta - 1)^2 + R_F \right] \cdot \omega_x$	$E_{nRGRF}^2 = \frac{2kT}{\pi} \left[ R_G (\beta - 1)^2 + R_F \left( \frac{1}{\hat{q}^2} - \frac{1}{q_p^2} \right) \right] \cdot \left( \frac{\pi}{2} q_p \omega_p \right) + \frac{2kT}{\pi} \left[ R_G (\beta - 1)^2 + R_F \right] \cdot \omega_x$	

<sup>a</sup> Quantity  $\hat{q} = q_p(\beta=0)$  is the pole Q of filter's passive-RC network and can be increased by the appropriate design [1].

Table 4. Component values and noise characteristics of design examples of second-order LP and BP-C filters as in Fig. 2(a) and (c) with  $\omega_p = 2\pi \cdot 86$  krad/s and  $q_p = 5$  (resistors in [kΩ], capacitors in [pF], noise in [μV],  $D_R$  in [dB])

No.	Filter\Design Parameter	Component values										Noise characteristics					
		r	ρ	$\hat{q}$	β	C <sub>1</sub>	C <sub>2</sub>	C <sub>TOT</sub>	R <sub>1</sub>	R <sub>2</sub>	R <sub>TOT</sub>	R <sub>1, R2</sub>	$e_{na}, i_{na1,2}$	R <sub>G, R<sub>F</sub></sub>	E <sub>no</sub>	D <sub>R</sub>	E <sub>no</sub> /β
1	Non Tapered	1	1	0.333	2.8	50	50	100	37	37	74	97.2	126	75.7	176.0	86.06	62.9
2	Capacitively Tapered	1	4	0.333	1.4	80	20	100	46.3	46.3	92.5	76.9	62.9	25.2	102.5	90.76	73.2
3	Resistively Tapered	4	1	0.333	5.6	50	50	100	18.5	74	92.5	194.3	251.5	171.1	360.9	79.82	64.5
4	Ideally Tapered	4	4	0.444	2.05	80	20	100	23.1	92.5	115.6	97.46	72.70	39.0	127.7	88.85	62.3
5	Cap-Taper and min. GSP	1.85	4	0.397	1.58	80	20	100	34.02	62.9	96.94	79.31	61.14	27.7	103.9	90.64	65.9

Table 5. Component values and noise characteristics of design examples of second-order HP and BP-R filters as in Fig. 2(b) and (d) with  $\omega_p = 2\pi \cdot 86$  krad/s and  $q_p = 5$  (resistors in [kΩ], capacitors in [pF], noise in [μV],  $D_R$  in [dB])

No.	Filter\Design Parameter	Component values										Noise characteristics					
		r	ρ	$\hat{q}$	β	C <sub>1</sub>	C <sub>2</sub>	C <sub>TOT</sub>	R <sub>1</sub>	R <sub>2</sub>	R <sub>TOT</sub>	R <sub>1, R2</sub>	$e_{na}, i_{na1,2}$	R <sub>G, R<sub>F</sub></sub>	E <sub>no</sub>	D <sub>R</sub>	E <sub>no</sub> /β
1	Non Tapered	1	1	0.333	2.8	50	50	100	37	37	74	137.9	126	75.8	201.6	84.88	72.0
2	Capacitively Tapered	1	4	0.333	5.6	80	20	100	46.3	46.3	92.5	344.7	252	171.4	460.1	77.71	82.2
3	Resistively Tapered	4	1	0.333	1.4	50	50	100	18.5	74	92.5	68.9	63.0	25.3	96.73	91.26	69.1
4	Ideally Tapered	4	4	0.444	2.05	80	20	100	23.1	92.5	115.6	109.2	72.8	39.1	137.0	88.24	66.8
5	Res-Taper and min. GSP	4	1.85	0.397	1.58	65	35	100	19.4	77.6	97.0	74.5	61.2	27.8	100.3	90.94	63.7

It is shown in [1] that there are various ways of impedance tapering a circuit. By application of various impedance scaling factors in (6) the resulting component values of the different types of tapered LP (and BP-C) circuits are listed in Table 4, and the components of HP (and BP-R) filters are listed in Table 5. The corresponding transfer function magnitudes are shown in Fig. 4.

A multi-parametric sensitivity analysis was performed on the filter examples in Tables 4 and 5 with the resistor and capacitor values assumed to be uncorrelated random variables, with zero-mean and 1% standard deviation. The

standard deviation  $\sigma_\alpha(\omega)$ [dB] of the variation of the logarithmic gain  $\Delta\alpha = 8.68588 \cdot \Delta|T(\omega)|/|T(\omega)|$  [dB] was calculated, with respect to all passive components, and plotted for the cases in Tables 4 and 5 in Fig. 5. There exist four different plots for all four Biquads in Fig. 2.

It is shown in Fig. 5(a) and (c) that the LP and BP-C filters no. 2, i.e. the capacitively-tapered filters with equal resistors ( $\rho=4$  and  $r=1$ ) have the minimum sensitivity to passive component variations [1]. The next best result is obtained with filter no. 5, i.e. the capacitively-tapered filter with minimum Gain-Sensitivity-Product (GSP).

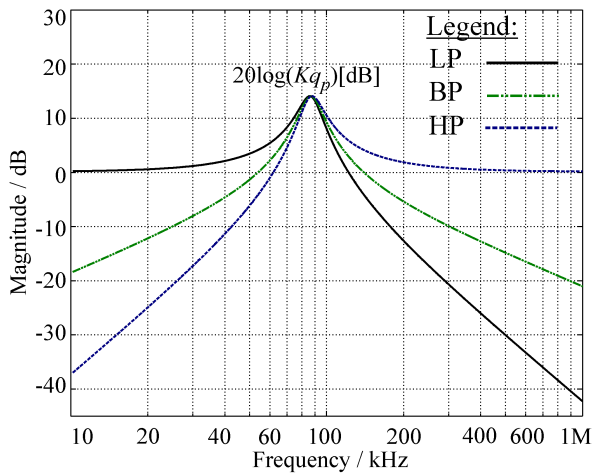


Fig. 4. Transfer function magnitudes of LP, HP and BP second-order filter examples [with (11) and  $K=1$ ]

It is shown in Fig. 5(b) and (d) that the HP and BP-R filters no. 3, i.e. the resistively-tapered filters with equal resistors (having component values in the third row in Table 5) have the minimum sensitivity to passive component variations. The next best result is 'optimum' design no. 5.

To conclude, the sensitivity curves in Fig. 5 confirm that complementary Biquads have identical optimum design, whereas dual Biquads have dual optimum designs. All complementary and dual Biquads in Fig. 2 have *identical* sensitivity figure of merit (all corresponding Schoeffler sensitivity curves in Fig. 5 are equally high).

The output noise spectral density [see eq. (3)], for these filters is shown in Fig. 6. Note that there exist two plots one for both the (complementary) LP and BP-C filters, because they have identical noise properties, and other for HP and BP-R filters.\* For these filters the total rms output noise voltage  $E_{no}$  [see eq. (4)], and the corresponding dynamic range  $D_R$  defined by (5) were calculated and are listed in Tables 4 and 5. The individual contributions to the 'active noise' are presented in separate columns. All these contributions, as well as the total output noise power are calculated using expressions in Table 3, and double-checked by numerical integrations of curves in Fig. 6 using Matlab.

Observing the  $E_{no}$  column in Table 4 and the noise spectral density in Fig. 6(a) we conclude that the LP and BP-C filters with the lowest output noise and maximum dynamic range are again filters no. 2. The second best results are obtained with filters no. 5, and these results are the same as those for minimum sensitivity shown above.

\*All noise spectral density plots have the same shape, which is dependent only on the denominator  $D(s)$  of the transfer function (8) and on the passive-RC-feedback-network denominator  $\hat{d}(s) = D(s, \beta = 0)$ , having maximum in the vicinity of the pole frequency  $\omega_p$ , i.e. it is invariant of coming from LP, HP or BP filters (see [9, 10]).

Analysis results in Table 5 and Fig. 6(b) show that designs no. 3 and no. 5 of the HP and BP-R filters have best noise performance, as well as minimum sensitivity.

The noise analysis above confirms that complementary circuits have *identical* noise properties, and on the other hand, those related by the RC-CR duality have *different* noise properties. Thus, there is a difference between LP and its dual counterpart HP filter in an output noise value. It is seen in Fig. 6 that in all design examples the noise of the HP filter is larger than that of the LP filter.

Consider, for example, two dual filters no. 1 in Tables 4 and 5, that are designed in the same way (with interchanging roles of  $r$  and  $\rho$ ) both having identical design parameters and component values, such as the same  $\beta$ ,  $\omega_p$ ,  $q_p$ ,  $R_{TOT}$ ,  $C_{TOT}$ , etc. Observing the individual noise contributions in Table 4 we see that the resistors  $R_1$  and  $R_2$  in the LP and BP-C Biquads contribute with  $97.2 \mu V$  ('passive noise') in the total of  $176 \mu V$  output noise. In the case of HP and BP-R Biquads in Table 5 we see that resistors  $R_1$  and  $R_2$  contribute with  $137.9 \mu V$  in the total of  $201.66 \mu V$  output noise. The reason for this lays in different *noise transfer functions* of the dual circuits in Fig. 3(a) and (b), from which the expressions in Table 3 are derived. In the first line in Table 3, and with (6), it is seen that between LP and HP filters there exists a difference in 'passive noise' by a factor  $(1+1/\rho)^\dagger$ . Another difference in the 'active noise' contributions due to  $i_{na1}$  can be neglected because  $i_{na1}$  is very small. The 'active noise' contributions are, therefore, *identical* for dual filters.

Consequently, we propose to use the LP and BP-C Biquads in Fig. 2(a) and (c) as recommended second-order active filter building blocks, because they have better noise figure-of-merit, and the HP Biquad in Fig. 2(b) as a second-order active filter building block for high-pass filters, if low noise and sensitivity properties are wanted. Unfortunately, it is unavoidable, that HP realizations will have a little bit worse noise performance.

### 3.2 Input Noise Optimization

When recovering low-level signals from a noisy background, an increase in output signal-to-noise ratio (SNR) is more important than a reduction of output noise. To increase the SNR, the output signal, divided by the rms output noise, must be maximized. The output signal is maximized when the gain  $K$  is maximized with  $\alpha=1$ , i.e.  $K=\beta$ ; which is assumed throughout of this paper. Furthermore, when comparing the SNR in the two design examples we must consider the maximum output-signal peak voltage delivered from the two circuits. Thus, to obtain a comparable

<sup>†</sup>In the design strategy no. 1 ( $r = 1$  and  $\rho = 1$ ), the 'passive noise' rms voltage (due to resistors  $R_1$  and  $R_2$ ) of HP filter is  $\sqrt{1 + 1/\rho} = \sqrt{2}$  times larger than that of the LP filter, i.e.  $137.9 \mu V / 97.2 \mu V = \sqrt{2}$ .

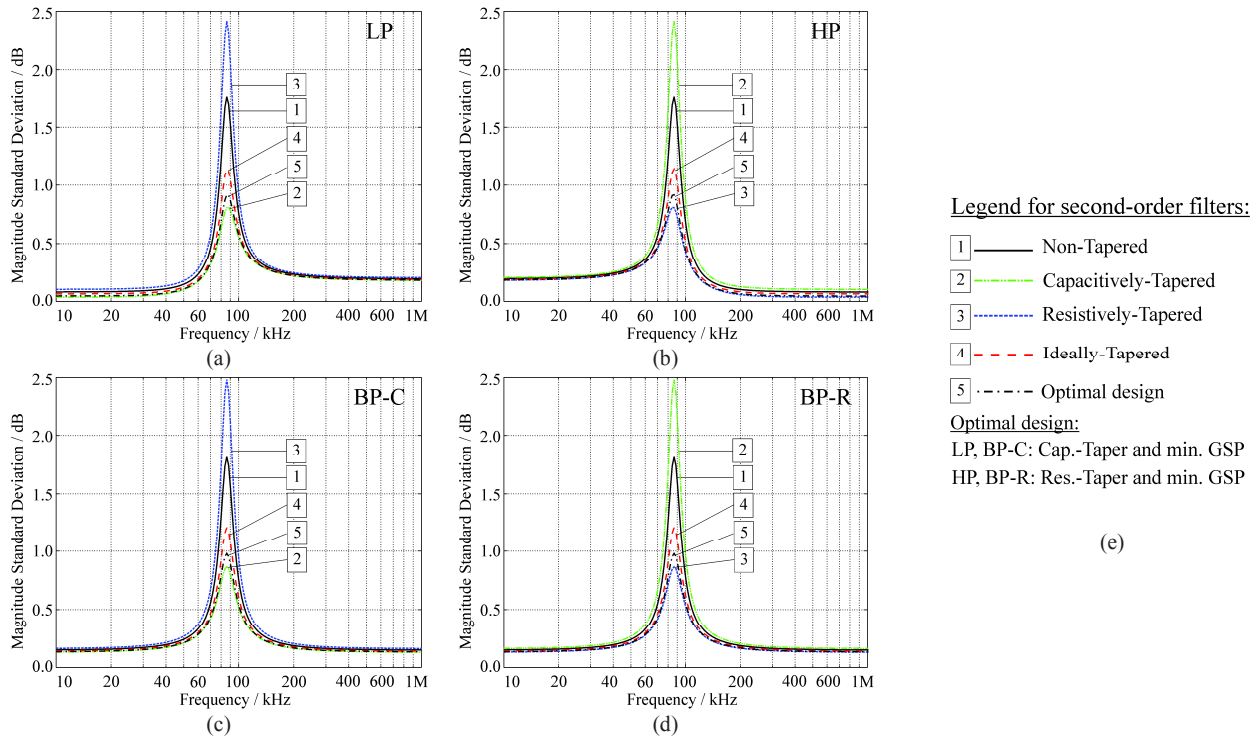


Fig. 5. Schoeffler sensitivities of second-order (a) LP, (c) BP-C filter examples given in Table 4, (b) HP, (d) BP-R filter examples given in Table 5, and (e) legend

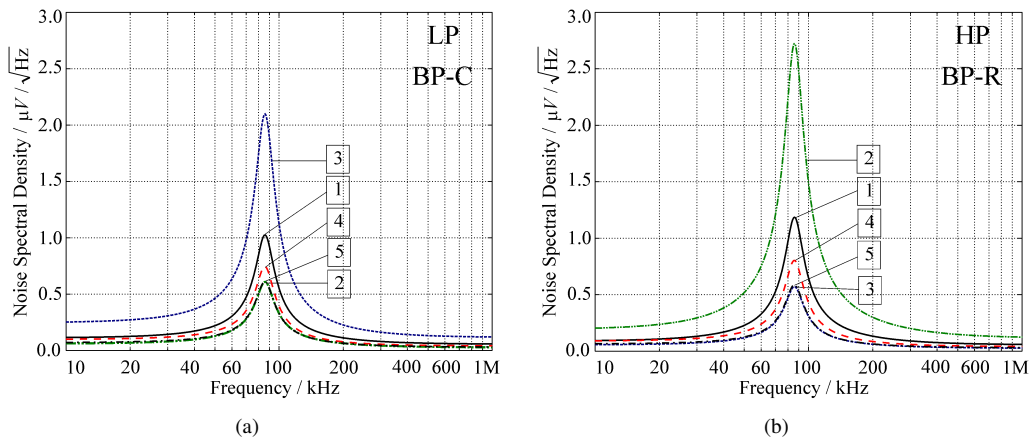


Fig. 6. Output noise spectral densities of second-order (a) LP/BP-C and (b) HP/BP-R filter examples given in Tables 4 and 5

quantities, the total output rms noise must be divided by the factor  $\beta$ . The resulting normalized output rms noise  $E_{no}/\beta$  (also referred to as 'input noise') is shown in the last columns in tables in this paper. Analysis results show that the improvement of 'output noise' is followed by the improvement of 'input noise', as well.

#### 4 THIRD-ORDER BI-TRIPLETS

The extension to third-order filter sections follows precisely the same principles as those above. Although the third-order LP filter has only one additional resistor the analysis is considerably more complicated. Moreover, unlike with second-order filters, third-order filters cannot be ideally tapered; instead only capacitive or resistive taper-

ing is possible [1].

Consider the third-order filter sections (Bitriplets) that realize LP and HP transfer functions, shown in Fig. 7. Optimum design of those filters for both low *passive and active* sensitivities is given in [2] and in Table 6. In [6] the detailed noise analysis on the analytical basis is given for the third-order LP filter circuit in Fig. 7(a). Here those results are extended to the optimum design of the (dual) HP filter circuit in Fig. 7(b).

Voltage transfer functions for the filters in Fig. 7 are given by:

$$T(s) = \frac{V_2}{V_1} = K \cdot \frac{n(s)}{s^3 + a_2s^2 + a_1s + a_0}, \quad (12a)$$

where numerators  $n(s)$  are given by:

$$n_{HP}(s) = s^3, \quad n_{LP}(s) = a_0. \quad (12b)$$

Coefficients  $a_i$  ( $i=0, 1, 2$ ), and gain  $K$  as functions of filter components are given in Table 7.

An optimization of both sensitivity *and* noise performance is possible by varying the general impedance scaling factors of the resistors and capacitors in the passive network of the filters in Fig. 7 (see [1]):

$$\begin{aligned} R_1 &= R, \quad R_2 = r_2R, \quad R_3 = r_3R, \\ C_1 &= C, \quad C_2 = C/\rho_2, \quad C_3 = C/\rho_3. \end{aligned} \quad (13)$$

The quantity referred to as 'design frequency' is defined by  $\omega_0 = 1/(RC)[1]$ .

To provide illustrative examples, consider the following filter specifications with edge frequencies 75/300 and attenuations  $A_{\max} = 0.5$ ,  $A_{\min} = 38$  (frequencies in kHz, loss in dB), which are satisfied by a third-order Chebyshev LP prototype filter [3]. The normalized poles readily follow using Matlab or from tables (e.g. in [14]) and are given by:

$$\begin{aligned} p_0 &= -\sigma_0 = -0.626456, \\ p_1, p_1^* &= -\sigma_1 \pm j\Omega_1 = -0.313228 \pm j1.02193. \end{aligned} \quad (14)$$

The corresponding normalized pole parameters are  $\omega_p=1.06885$ ,  $q_p=1.70619$  and  $\gamma=0.626456$ . To design LP filter the frequencies  $\omega_p$  and  $\gamma$  are multiplied by the pass-band cut-off frequency  $\omega_c=2\pi \cdot 75$  krad/s, and using the relations in the first column in Table 7, the denormalized coefficients  $a_i$  ( $i=0, 1, 2$ ) of the third-order LP transfer function are given by:

$$\begin{aligned} a_0 &= 4.79326 \cdot 10^{18}, \\ a_1 &= 5.45357 \cdot 10^{12}, \\ a_2 &= 2.36169 \cdot 10^6. \end{aligned} \quad (15)$$

To design HP filter the LP-HP frequency transformation transforms the frequencies  $\omega_p$  and  $\gamma$ . First, they are inverted and then multiplied by the HP pass-band cut-off frequency  $\omega_c=2\pi \cdot 300$  krad/s. Finally, the denormalized coefficients  $a_i$  ( $i = 0, 1, 2$ ) of the third-order HP transfer function are given by:

$$\begin{aligned} a_0 &= 9.35785 \cdot 10^{18}, \\ a_1 &= 6.22008 \cdot 10^{12}, \\ a_2 &= 4.04252 \cdot 10^6. \end{aligned} \quad (16)$$

The magnitudes of the LP and HP transfer function are shown in Fig. 8 together with filter specifications.

In Tables 8 and 9 various non-optimized and optimized filter examples are listed in terms of filter sensitivity to component tolerances. In order to compare the different circuits with regard to their noise performance, the total capacitance for each is held constant, i.e.  $C_{TOT} = 300$  pF. In the first two lines there are simple equal-resistor and equal-capacitor filters which are considered as non-optimized examples. For practical reasons, to be comparable with other examples,  $\beta$  is chosen equal to 2.

Some of various ways of impedance tapering circuits such as those given in Fig. 7 are based on 'partial impedance tapering' with a different parameter  $\omega_0$  (i.e. capacitive tapering for LP and resistive for HP filter). In Tables 8 and 9 they are listed as tapered circuits no. 3, 4 and 5. The circuit no. 4 is calculated in an *optimum way* using step-by-step design procedure proposed in Table 6.

A multi-parametric Schoeffler sensitivity analysis was performed and the output noise spectral density was calculated for these filters using Matlab. Results for LP and HP filters are shown in Fig. 9 and 10, respectively.

As shown in Fig. 9(a) and 10(a), the 'optimal' circuit no. 4 has a significantly lower sensitivity to component tolerances than all the other circuits, especially the non-optimized circuits no. 1 and 2. For the filters in Tables 8 and 9 the total rms output noise voltage  $E_{no}$ , and the corresponding dynamic range  $D_R$  defined by (5) were calculated and presented. The individual contributions to the 'active noise' are presented in separate columns.

From Fig. 9(b) and 10(b) and the  $E_{no}$  columns we conclude that the filter with the lowest output noise and maximum dynamic range is again filter no. 4. This circuit has a significantly lower total output noise than all the other circuits, as well as the minimum sensitivity to component tolerances. It also has very low input noise and SNR: see the  $E_{no}/\beta$  columns in Tables 8 and 9. Thus, the minimum-noise and minimum-sensitivity designs coincide. The circuit with the poorest performance with regard to both sensitivity and noise is the filter no. 2 in both LP and HP cases.

If we compare the output noise of two third-order dual circuits we see again that HP filter has *larger* noise than LP

Table 6. Optimum step-by-step design procedure for third-order filters in Fig. 7

(a) LP	(b) HP
i) Choose: $\rho_2=\rho, \rho_3=\rho^2$ (e.g. $\rho=3$ ).	i) Choose: $r_2=r, r_3=r^2$ (e.g. $r=3$ ).
ii) Choose: $\omega_0$ ; $\omega_0 < \omega_{0\max}$ , where $\omega_{0\max}$ is defined by: $\omega_0^3 - a_2\omega_0^2 + a_1\omega_0 - a_0 = 0 \rightarrow \omega_a$ $\omega_{D1} = 4a_0 / (4a_1 - a_2^2) \rightarrow \omega_{0\max} = \min\{\omega_a, \omega_{D1}\}.$	ii) Choose: $\omega_0$ ; $\omega_0 > \omega_{0\min}$ , where $\omega_{0\min}$ is defined by: $\omega_0^3 - a_2\omega_0^2 + a_1\omega_0 - a_0 = 0 \rightarrow \omega_a$ $\omega_{D1} = (4a_0a_2 - a_1^2) / 4a_0 \rightarrow \omega_{0\min} = \max\{\omega_a, \omega_{D1}\}.$
iii) Calculate $a, b, c$ : $\alpha_0 = a_0 / \omega_0^3; \alpha_1 = a_1 / \omega_0^2; \alpha_2 = a_2 / \omega_0 \rightarrow$ $a = \alpha_0 + \alpha_2 - \alpha_1 - 1; b = \alpha_2 - 2; c = -(1 + \rho_2).$	iii) Calculate $a, b, c$ : $\alpha_0 = a_0 / \omega_0^3; \alpha_1 = a_1 / \omega_0^2; \alpha_2 = a_2 / \omega_0 \rightarrow$ $a = (1/\omega_0)(-a_0 - a_2 + a_1 + 1); b = a_1/\omega_0 - 2; c = -(1 + r_2).$
iv) Calculate $r_2$ : $ar_2^2 + br_2 + c = 0 \rightarrow r_2$ (take positive and real $r_2$ ).	iv) Calculate $\rho_2$ : $a\rho_2^2 + b\rho_2 + c = 0 \rightarrow \rho_2$ (take positive and real $\rho_2$ ).
v) Calculate $r_3$ : $r_3 = \rho_2\rho_3 / (r_2\alpha_0)$ (In the step ii) above $\omega_0$ should be chosen to provide $r_2 \approx r_3$ for min. sensitivity).	v) Calculate $\rho_3$ : $\rho_3 = r_3r_2\alpha_0 / \rho_2$ (In the step ii) above $\omega_0$ should be chosen to provide $\rho_2 \approx \rho_3$ for min. sensitivity).
vi) Calculate $\beta$ : $\beta = 1 + \frac{\rho_2}{\rho_3} - \frac{r_3}{\rho_3} \left[ (\alpha_2 - 1) - \frac{1 + \rho_2}{r_2} \right]$	vi) Calculate $\beta$ : $\beta = 1 + \frac{r_2}{r_3} \left[ \frac{\rho_3 + r_3(1 - \alpha_2)}{\rho_2 + 1} + 1 \right]$
vii) Choose $C_1$ [or calculate $C_1 = C_{TOT} / (1 + 1/\rho_2 + 1/\rho_3)$ ] and calculate $R_1 = (\omega_0 C_1)^{-1}$ .	vii) Choose $C_1$ [or calculate $C_1 = C_{TOT} / (1 + 1/\rho_2 + 1/\rho_3)$ ] and calculate $R_1 = (\omega_0 C_1)^{-1}$ .
viii) Choose $R_G$ and calculate remaining filter components: $C_2 = C_1 / \rho_2; C_3 = C_1 / \rho_3; R_2 = r_2 R_1; R_3 = r_3 R_1;$ $a = K / \beta; R_{11} = R_1 / \alpha; R_{12} = R_1 / (1 - \alpha); R_F = R_G (\beta - 1).$	viii) Choose $R_G$ and calculate remaining filter components: $R_2 = r_2 R_1; R_3 = r_3 R_1; C_2 = C_1 / \rho_2; C_3 = C_1 / \rho_3;$ $a = K / \beta; C_{11} = \alpha C_1; C_{12} = (1 - \alpha) C_1; R_F = R_G (\beta - 1).$

Table 7. Transfer function coefficients of third-order active-RC filters with positive feedback in Fig. 7

Coefficient	(a) LP	(b) HP
$a_0 = \gamma\omega_p^2$	$(R_1 R_2 R_3 C_1 C_2 C_3)^{-1}$	$(R_1 R_2 R_3 C_1 C_2 C_3)^{-1}$
$a_1 = \omega_p^2 + \frac{\gamma\omega_p}{q_p}$	$\frac{R_1 C_1 + (R_1 + R_2 + R_3) C_3 + (1 - \beta) C_2 (R_1 + R_2)}{R_1 R_2 R_3 C_1 C_2 C_3}$	$\frac{R_1 (C_1 + C_2) + R_2 (C_2 + C_3) + R_3 C_3 (1 - \beta)}{R_1 R_2 R_3 C_1 C_2 C_3}$
$a_2 = \gamma + \frac{\omega_p}{q_p}$	$\frac{R_1 R_2 C_1 C_3 + R_1 R_3 C_3 (C_1 + C_2) + R_2 R_3 C_2 C_3 + (1 - \beta) R_1 R_2 C_1 C_2}{R_1 R_2 R_3 C_1 C_2 C_3}$	$\frac{R_1 R_2 C_1 (C_2 + C_3) + R_2 C_2 C_3 (R_1 + R_3) + R_1 R_3 C_3 (C_1 + C_2) (1 - \beta)}{R_1 R_2 R_3 C_1 C_2 C_3}$
$K$	$\alpha\beta$	$\alpha\beta$

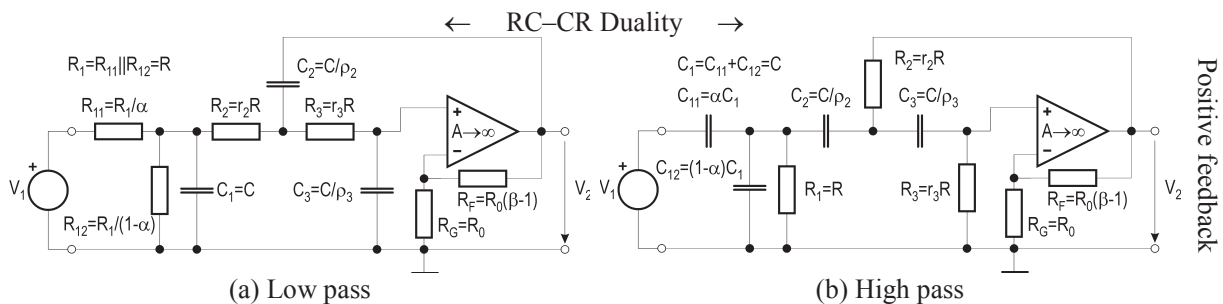


Fig. 7. Third-order LP and HP active-RC filters with impedance scaling factors  $r_i$  and  $\rho_i$  ( $i=2, 3$ )

filter, although their sensitivities are *identical*. The reason is twofold: *i*) different noise transfer functions (as in the second-order case), and *ii*) the HP filter in this example has larger  $\omega_p$ . Detailed analytical investigation of the noise in the third-order filters in [6] shows that the output noise is

proportional to  $\omega_p$  (as in the second-order case), which in turn is proportional to the cut-off frequency  $\omega_c$ , determined by the filter specifications.

Table 8. Component values and noise characteristics of design examples of third-order LP filter as in Fig. 7(a) and (15) (resistors in [kΩ], capacitors in [pF], noise in [μV],  $D_R$  in [dB])

No.	Filter/Design Parameter	Component values										Noise characteristics					
		$\omega_0 \cdot 10^3$	$r_2$	$r_3$	$\rho_2$	$\rho_3$	$\beta$	$C_1$	$C_{TOT}$	$R_1$	$R_{TOT}$	$R_1, R_2, R_3$	$e_{na}, i_{na1,2}$	$R_G, R_F$	$E_{no}$	$D_R$	$E_{no}/\beta$
1	Equal Resistors	205.5	1	1	2.31	3.74	2.0	176.4	300	27.60	82.8	53.07	68.62	36.42	94.1	91.5	47.0
2	Equal Capacitors	251.0	1.48	0.14	1	1	2.0	100	300	39.84	104.6	50.47	132.2	70.18	158.0	87.0	79.0
3	Capacitively Tapered	200.0	1.04	2.78	3	9	1.92	207.7	300	24.07	115.9	66.43	57.23	29.72	92.6	91.6	48.3
4		260.0	2.60	2.43	3	9	1.41	207.7	300	18.52	111.8	46.31	43.44	17.51	65.9	94.6	46.9
5		290.0	8.54	1.03	3	9	1.27	207.7	300	16.60	175.4	58.42	72.88	25.17	96.7	91.3	76.3

Table 9. Component values and noise characteristics of design examples of third-order HP filter as in Fig. 7(b) and (16) (resistors in [kΩ], capacitors in [pF], noise in [μV],  $D_R$  in [dB])

No.	Filter/Design Parameter	Component values										Noise characteristics					
		$\omega_0 \cdot 10^6$	$r_2$	$r_3$	$\rho_2$	$\rho_3$	$\beta$	$C_1$	$C_{TOT}$	$R_1$	$R_{TOT}$	$R_1, R_2, R_3$	$e_{na}, i_{na1,2}$	$R_G, R_F$	$E_{no}$	$D_R$	$E_{no}/\beta$
1	Equal Capacitors	4.323	2.31	3.74	1	1	2.0	100	300	2.313	16.3	56.89	134.7	71.5	162.8	86.74	81.38
2	Equal Resistors	3.537	1	1	1.48	0.14	2.0	34.58	300	8.177	24.53	123.7	264.7	140.5	324.3	80.75	162.1
3	Resistively Tapered	4.442	3	9	1.04	2.78	1.92	129.1	300	1.744	22.66	57.90	110.4	57.4	137.2	88.22	71.47
4		3.411	3	9	2.60	2.43	1.41	167.3	300	1.752	22.78	40.36	82.4	33.2	97.6	91.18	69.50
5		3.060	3	9	8.54	1.03	1.27	143.8	300	2.272	29.54	73.92	137.6	47.5	163.3	86.71	128.7

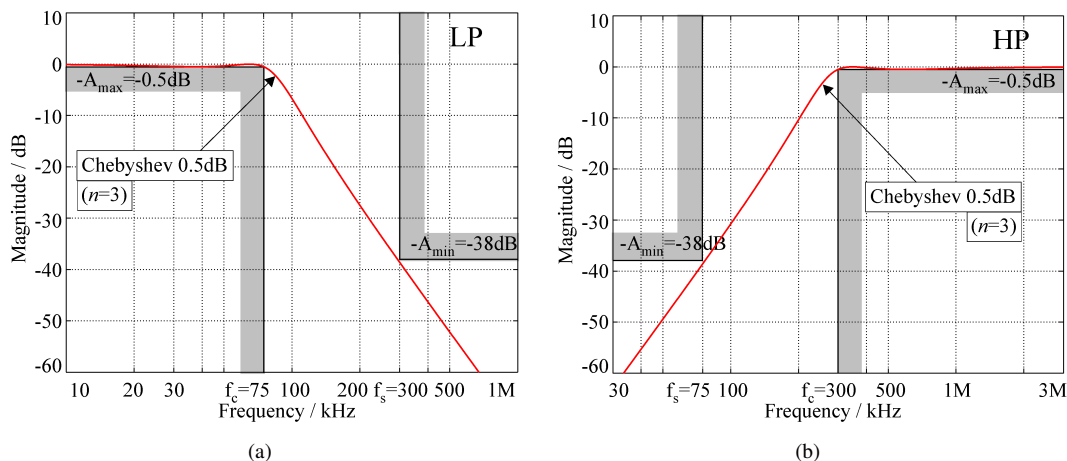


Fig. 8. Filter specifications and transfer function magnitudes of third-order filter examples. (a) LP [with (15) and  $K=1$ ]. (b) HP [with (16) and  $K=1$ ]

### 5 CONCLUSION

In this paper we demonstrate that LP, BP and HP allpole active-RC filters of second- and third-order that are designed in [2] for minimum sensitivity to component tolerances, are also superior in terms of low output thermal noise when compared with standard designs. The filters are of low power because they use only one opamp.

What we show here is that second-order, allpole, single-amplifier LP/HP filters with positive feedback using capacitive/resistive (or ideal) impedance tapering in order to minimize sensitivity to component tolerances also mini-

mizes the output (or input) thermal noise. The second-order BP-C filter with negative feedback is recommended filter block when the low noise is required.

The same is shown for low-sensitivity, third-order, LP and HP filters of the same topology. Using low-noise opamps and metal-film small-valued resistors together with the proposed design method, low-sensitivity and low-noise filters result simultaneously. The mechanism by which the sensitivity to component tolerances of the LP, HP and BP allpole active-RC filters is reduced, also efficiently reduces the total noise at the filter output and the noise referred to the filter input.

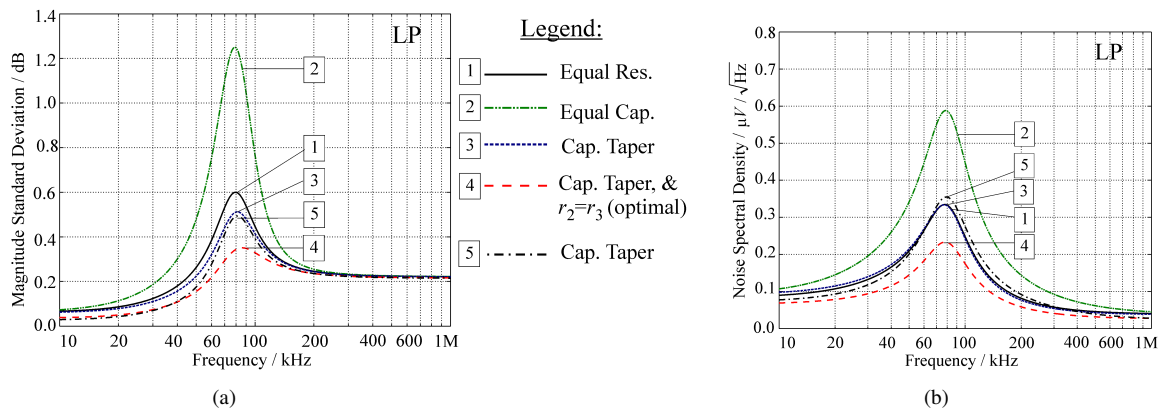


Fig. 9. Schoeffler sensitivities and output noise spectral densities of third-order LP filter examples given in Table 8

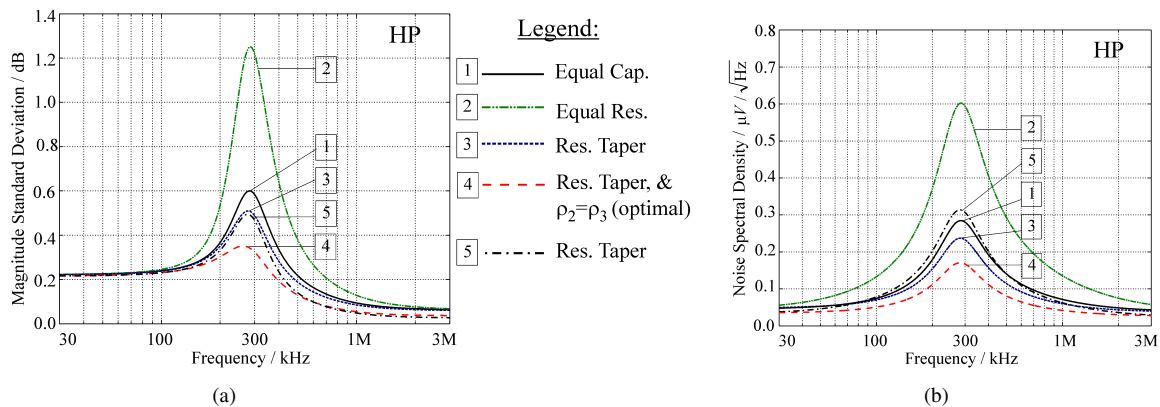


Fig. 10. Schoeffler sensitivities and output noise spectral densities of third-order HP filter examples given in Table 9

REFERENCES

[1] G. S. Moschytz, “Low-Sensitivity, Low-Power, Active-RC Allpole Filters Using Impedance Tapering,” *IEEE Trans. on Circuits and Systems*, vol. CAS-46, no. 8, pp. 1009–1026, Aug. 1999.

[2] D. Jurišić, G. S. Moschytz and N. Mijat, “Low-Sensitivity Active-RC Allpole Filters Using Optimized Biquads,” *Automatika*, vol. 51, no. 1, pp. 55–70, Mar. 2010.

[3] D. Jurišić, G. S. Moschytz and N. Mijat, “Low-Sensitivity, Single-Amplifier, Active-RC Allpole Filters Using Tables,” *Automatika*, vol. 49 no. 3-4, pp. 159–173, Nov. 2008.

[4] D. Jurišić and G. S. Moschytz, “Low Noise Active-RC Low-, High- and Band-pass Allpole Filters Using Impedance Tapering,” in *Proceedings of MELeCon 2000*, Lemesos, Cyprus, May 29-31, 2000., pp. 591–594.

[5] D. Jurišić, *Active RC Filter Design Using Impedance Tapering*. Zagreb, Croatia: Ph. D. Thesis, University of Zagreb, April 2002.

[6] D. Jurišić, G. S. Moschytz and N. Mijat, “Low-Noise, Low-Sensitivity, Active-RC Allpole Filters Using Impedance Tapering,” *International Journal of Circuit Theory and Applications*, n/a. doi: 10.1002/cta.740.

[7] L. T. Bruton, F. N. Trofimenkoff, and D. H. Treleaven, “Noise Performance of Active-RC Filters,” *IEEE J. Solid-State Circuits*, vol. SC-8, no. 1, pp. 85–91, Feb. 1973.

[8] F. N. Trofimenkoff, D. H. Treleaven and L. T. Bruton, “Noise Performance of RC-Active Quadratic Filter Sections,” *IEEE Trans. Circuit Theory*, vol. CT-20, no. 5, pp. 524–532, Sept. 1973.

[9] H. J. Baechler and W. Guggenbuehl, “Noise and Sensitivity Optimization of a Single-Amplifier Biquad,” *IEEE Trans. on Circuits and Systems*, vol. CAS-26, no. 1, pp. 30–36, Jan. 1979.

[10] H. J. Bächler and W. Guggenbühl, “Noise and Sensitivity Performance of Complementary and Dual Second Order Active Filter Building Blocks,” in *Proceedings of ECCTD-78*, Lausanne, Switzerland, Sept. 4–8, 1978, pp. 256–260.

[11] N. Stojković and N. Mijat, “Noise and Dynamic Range of Second Order OTA-C BP Filter Sections,” in *Proceedings of ECCTD-99*, Stresa, Italy, Aug. 29–Sept. 2, 1999, pp. 795–798.

- [12] G. S. Moschytz, *Linear Integrated Networks: Design*. New York (Bell Laboratories Series): Van Nostrand Reinhold Co., 1975.
- [13] R. P. Sallen and E. L. Key, "A practical Method of Designing RC Active Filters," *IRE Trans. on Circuit Theory*, vol. CT-2, pp. 74–85, Mar. 1955.
- [14] G. S. Moschytz and P. Horn, *Active Filter Design Handbook*. Chichester, UK.: John Wiley and Sons, 1981. (IBM Progr. Disk: ISBN 0471-915 43 2)



**Dražen Jurišić** is assistant professor of the Faculty of Electrical Engineering at the University of Zagreb in Croatia where he received his B.Sc., M.Sc. and Ph.D. degrees in Electrical Engineering in 1990, 1995 and 2002, respectively. In 2005 he was elected as assistant professor. He is involved in teaching lectures in undergraduate courses on "Electrical circuits", "Signals and systems" and "Analog and mixed signal processing circuitry". Present interests include analog and digital signal processing and filter design. He

worked as a researcher on the three scientific projects supported by Ministry of Science and Technology, Republic of Croatia. From 1997 until 1999 he was with Swiss Federal Institute of Technology (ETH) Zürich, Switzerland, as holder of Swiss Federal Scholarship for Foreign Students doing Ph.D. research in the field of analog active-RC filters. He was rewarded with the silver plaque "Josip Loncar" for his Ph.D. thesis. He is a member of KoREMA and IEEE-CAS society. He speaks English and German.



**George S. Moschytz** is head of the Electrical and Computer Engineering Department at the Bar-Ilan University in Israel. Present interests include analog and digital, sampled-data, and adaptive filters, for communication systems. Earlier Professor Moschytz was with RCA Labs in Zürich, Bell Telephone Labs, Holmdel, NJ, where he supervised a group designing analog and digital integrated circuits for data communications, and at ETH, Zürich, as Professor and Director of the Institute for Signal and Information Processing.

Author of "Linear Integrated Networks: Fundamentals" and "Linear Integrated Networks: Design", and co-author of the "Active Filter Design Handbook", and "Adaptive Filter" (in German). Editor of "MOS Switched-Capacitor Filters: Analysis and Design", and co-editor of "Tradeoffs in Analog Design". Authored many papers in the field of network theory, design, and analysis, and holds numerous patents in these areas. Professor Moschytz has held the position of president of the IEEE Circuit and Systems Society, and is an elected member of the Swiss Academy of Engineering Sciences. He is a Life-Fellow of the IEEE, and has received several IEEE awards, including the IEEE CAS Education Award.



**Neven Mijat** received his B.Sc., M.Sc. and Ph.D. degrees in Electrical Engineering from the Faculty of Electrical Engineering, University of Zagreb in 1970, 1974 and 1984, respectively. In 1970 he joined the Department of Electronic Systems and Information Processing at the Faculty of Electrical Engineering, University of Zagreb, where he is currently professor within the Networks, Systems and Signals group. At the Faculty he is involved in teaching lectures in undergraduate courses involving Network Theory, Fil-

ters, Analogue circuits, SC circuits, and in the postgraduate courses "Filter design", and "Numerical methods in system design". His current research interests include data acquisition systems and filter theory and realization methods. He was also leading a number of R&D projects. He is member of IEEE, CROMBES, KoREMA and some other professional societies. He was a principal investigator for few scientific projects and development projects for companies. He received the "Josip Loncar" silver plaques for his M.Sc. and Ph.D. theses in 1974 and 1984 respectively.

#### AUTHORS' ADDRESSES

**Asst. Prof. Dražen Jurišić, Ph.D.**

**Prof. Neven Mijat, Ph.D.**

**Department of Electronic Systems and Information Processing,**

**Faculty of Electrical Engineering and Computing,**

**University of Zagreb,**

**Unska 3, 10000, Zagreb, Croatia**

**email: drazen.juriscic@fer.hr , neven.mijat@fer.hr**

**Prof. George S. Moschytz, Ph.D.**

**School of Engineering,**

**Bar-Ilan University, Ramat-Gan, 52900, Israel**

**email: moschytz@isi.ee.ethz.ch**

Received: 2010-08-27

Accepted: 2010-11-10